

JPET #93922

## A Biosynthetic Pathway Generating 12-Hydroxy-5,8,14-eicosatrienoic Acid from Arachidonic Acid is Active in Mouse Skin Microsomes\*

Liping Du, Valery Yermalitsky, David L. Hachey, Setti G. Jagadeesh, John R. Falck, and Diane S. Keeney

VA Tennessee Valley Healthcare System, Nashville, TN 37212 (D.S.K.); Departments of Medicine/Dermatology (D.S.K.), Pharmacology (D.L.H.), and Biochemistry (L.D., V.Y., D.S.K.), Vanderbilt University School of Medicine, Nashville, TN 37232; and the Department of Biochemistry, University of Texas Southwestern Medical Center, Dallas, TX 75390 (S.G.J., J.R.F.)

---

JPET #93922

Running title: Epidermal 12-hydroxy-5,8,14-eicosatrienoic acid synthesis

Corresponding author address: Diane S. Keeney, PhD, Dept. Medicine/Dermatology & Biochemistry, Vanderbilt University, 607 Light Hall (0146), Nashville, TN 37232-0146  
USA

Email: [diane.keeney@vanderbilt.edu](mailto:diane.keeney@vanderbilt.edu)

Phone: 615-327-4751 ext. 5283

Fax: 615-322-4349

Text: 35 pages\_

References: 40 citations

Abstract: 247 words

Introduction: 552 words

Discussion: 1167 words

Tables: 1

Figures: 5

Abbreviations: EET, epoxyeicosatrienoic acid; DiHETrE, dihydroxyeicosatrienoic acid; HETE, hydroxyeicosatetraenoic acid; LC/ESI/MS, liquid chromatography negative electrospray ionization mass spectrometry; 12-HETrE, 12-hydroxy-5,8,14-eicosatrienoic acid; 15-HETrE, 15-hydroxy-8,11,13-eicosatrienoic acid; 12-HpETE, 12-hydroperoxy eicosatetraenoic acid; 12-oxo-ETE, 12-oxo-5,8,10,14-eicosatetraenoic acid; 12-oxo-ETrE, 12-oxo-5,8,14-eicosatrienoic acid.

Subject area: Metabolism

## Abstract

The epidermis expresses cyclooxygenases, lipoxygenases and cytochromes P450, which utilize arachidonic acid to generate a diverse array of lipid mediators affecting epidermal cellular differentiation and functions. Recent studies show that mouse epidermis expresses CYP2B19, a keratinocyte-specific epoxygenase that generates 11,12- and 14,15-epoxyeicosatrienoic (EET) acids from arachidonate. We studied CYP2B19-dependent metabolism in mouse epidermal microsomes, reconstituted in the presence of [1-<sup>14</sup>C]-arachidonic acid. The majority of the [<sup>14</sup>C]-products formed independently of NADPH, indicative of robust epidermal cyclooxygenase and lipoxygenase activities. We studied two NADPH-dependent products generated in a highly reproducible manner from arachidonate. One of these (product I) co-eluted with the CYP2B19 product 14,15-EET on a reversed-phase HPLC system; there was no evidence for other regioisomeric EET products. Further analyses proved that product I was not an epoxy fatty acid, based on different retention times on a normal phase HPLC system and failure of product I to undergo hydrolysis in acidic solution. We analyzed purified epidermal [<sup>14</sup>C]-products by liquid chromatography negative electrospray ionization mass spectrometry. Structures of the NADPH-dependent products were confirmed to be 12-oxo-5,8,14-eicosatrienoic acid (I) and 12-hydroxy-5,8,14-eicosatrienoic acid (II). This was the first evidence for a 12-hydroxy-5,8,14-eicosatrienoic acid biosynthetic pathway in mouse epidermis. Epidermal microsomes also generated 12-hydroperoxy, 12-hydroxy, and 12-oxo eicosatetraenoic acids from arachidonate, possible intermediates in the 12-hydroxy-5,8,14-eicosatrienoic

JPET #93922

acid biosynthetic pathway. These results predict hydroxyeicosatrienoic acids are synthesized from arachidonate in human epidermis. This would have important implications for human skin diseases given the known pro- and anti-inflammatory activities of stereo- and regioisomeric hydroxyeicosatrienoic acids.

## Introduction

Cyclooxygenases, lipoxygenases and cytochromes P450 (*CYP* gene products) activate arachidonic acid. Prostanoids, hydroxy and epoxy fatty acids generated by these enzyme systems mediate signals involved in epidermal homeostasis, skin diseases and cancers. These lipid mediators are implicated in mechanisms regulating diverse cellular processes including epidermal cell proliferation and differentiation, cutaneous responses to inflammation and environmental cell damage and cutaneous immune responses (recently reviewed by Ikai, 1999; Iversen and Kragballe, 2000; Marks et al., 2000; Ziboh et al., 2000; Kabashima and Miyachi, 2004).

In mouse skin, epidermal cyclooxygenases generate mainly prostaglandins E<sub>2</sub> and D<sub>2</sub> from arachidonate. 12-Hydroxyeicosatetraenoic acid (12-HETE) is the main hydroxy fatty acid generated (Hammarström et al., 1979; Bedford et al., 1983; Ruzicka et al., 1983), and levels of these enzyme activities are regulated as a function of the differentiation state of the epidermal cells (Henke et al., 1986; Cameron et al., 1990). In human skin, epidermal cyclooxygenases generate mainly prostaglandins E<sub>2</sub> and F<sub>2α</sub> from arachidonate. The main hydroxy fatty acids generated are 12- and 15-hydroxyeicosatetraenoic acids (12-/15-HETE), and the ratio of these regioisomers is influenced by the differentiation state of epidermal cells (reviewed: Iversen and Kragballe, 2000; Ziboh et al., 2000).

The cytochrome P450 superfamily includes 57 putatively functional *CYP* genes in humans (Nelson et al., 2004). *CYP* enzymes have critical roles in metabolism of diverse natural and foreign compounds (Nebert and Russell, 2002). Several are active

JPET #93922

towards arachidonate in *in vitro* studies--especially CYP1, 2, 3 and 4 family members. Arachidonic acid monooxygenases typically generate multiple products in a regio- and stereo-specific manner (Capdevila and Falck, 2002). In addition to epoxy- and  $\omega/\omega-1$  hydroxy fatty acids, they can catalyze *bis*-allylic oxidations such that in a given tissue 12- and 15-HETE regioisomers, for example, potentially arise from both lipoxygenase and CYP-dependent metabolism.

The biosynthesis and functions of CYP-derived eicosanoids in the skin are poorly understood even though this enzyme system likely generates a large number of biologically active lipid mediators in epidermal cells. Cytochromes P450 require electron transfer proteins to transfer electrons from NADPH to the enzyme active site. Hence, CYP-derived products are generally not observed under assay conditions used to study cyclooxygenase and lipoxygenase mediated metabolism. The first evidence that epidermal cells generate CYP-derived epoxyeicosatrienoic (EET) acids was obtained using human keratinocyte cell suspensions, in which cell membranes and reducing environment remained intact (Holtzman et al., 1989). Although analyte identity was not proven in these studies, mass spectrometry was used in a subsequent study to measure cellular levels of EETs arising from endogenous arachidonic acid, in both human and mouse epidermal cells (Ladd et al., 2003; Du et al., 2005). These results confirmed that catalytically active epoxygenases are expressed in epidermal cells since CYP enzymes are the only known catalytic source of EETs.

Previously we identified CYP2B19 as a major source of EET formation in mouse skin (Du et al., 2005). In the present study, we aimed to demonstrate that mouse epidermal microsomes generate EETs when reconstituted in the presence of [1-<sup>14</sup>C]-

JPET #93922

arachidonate. To further establish roles for CYP2B19, we aimed to compare the regio- and stereo-specificity of EETs formed by mouse epidermal microsomes with those generated by *E. coli*-expressed CYP2B19 (Keeney et al., 1998). Instead of CYP-derived EETs, we identified intermediates in a biosynthetic pathway not previously described in mouse skin that leads to formation of 12-hydroxy-5,8,14-eicosatrienoic acid (12-HETrE).

## Methods

**Microsomes preparation.** Full-thickness skin or epidermal sheets from newborn mice (CD-1 strain; Charles Rivers, Wilmington, MA) were homogenized in 0.05 M Tris-HCl pH 7.4 containing 0.25 M sucrose, 0.15 M KCl and protease inhibitors (Complete-mini, Roche Applied Science, Indianapolis, IN). Epidermal sheets were peeled from the dermis after a 3-h incubation at 4°C in 0.3% Dispase II (Sigma-Aldrich, St. Louis, MO), in phosphate buffered saline. Tissues were disrupted by three 1-min pulses at maximum speed ( $\approx 26,000$  rpm), using a Polytron PT3100 fitted with a 12-mm generator with knives (PT-DA3013/2TM; Brinkmann Instrument Inc., Westbury, NY). Samples were chilled for one minute between pulses. Homogenates were centrifuged for 20 min at 900 x *g* and 4°C. The 900 x *g* supernatants were centrifuged for 30 min at 12,000 x *g* and 4°C. The 12,000 x *g* supernatants were centrifuged for 60 min at 100,000 x *g* and 4°C. If not used immediately, the 100,000 x *g* microsomal pellets were overlaid with 1-ml of 30% glycerol in 0.05 M Tris-HCl pH 7.4 and frozen at -30°C for up to two months. Before use, the glycerol overlay was removed, and pellets were washed with 1-ml of 0.15 M KCl, 0.01 M MgCl<sub>2</sub>, 0.05 M Tris-HCl pH 7.4.

**Arachidonic acid metabolism assays.** [1-<sup>14</sup>C]-Arachidonic acid (48 mCi/mmol; Perkin Elmer Inc., Wellesley, MA) was purified by SiO<sub>2</sub> chromatography, and assays were performed at pH 7.4 and 35°C as described previously (Capdevila et al., 1990), with minor modifications. Microsomal pellets were resuspended directly in reaction buffer [0.15 M KCl, 0.01 M MgCl<sub>2</sub>, 0.05 M Tris-HCl pH 7.4, 2 mg/ml sodium isocitrate]

JPET #93922

and preincubated at 35°C for 15 min ( $\pm$  inhibitors). [1-<sup>14</sup>C]-Arachidonate substrate (70-100  $\mu$ M) was added 2-min prior to starting reactions with NADPH.

The extracted reaction products were reconstituted in initial phase solvent and resolved by reversed-phase HPLC (5- $\mu$ m Dynamax Microsorb C<sub>18</sub> column; 4.6  $\times$  250 mm; Varian Inc., Palo Alto, CA), using a linear solvent gradient from initially water/acetonitrile/acetic acid (49.95/49.95/0.1; v/v/v) to acetonitrile/acetic acid (99.9/0.1; v/v) in 40 min at 1 ml/min (Capdevila et al., 1990). Effluents were collected separately and resolved by normal phase HPLC (5- $\mu$ m Dynamax Microsorb silica column; 4.6  $\times$  250 mm; Varian Inc., Palo Alto, CA), using an isocratic solvent mixture of acetic acid/2-propanol/hexane (0.1/0.5/99.4; v/v/v) at 1.0 ml/min. Separations were performed using an Alliance Systems 2690 separation module and model 996 photodiode array detector (Waters Corp., Milford, MA). Quantitation of radiolabeled products utilized a  $\beta$ -RAM Model 3 radiochromatography detector fitted with a 250- $\mu$ l lithium glass scintillator solid cell (IN/US Systems Inc., Tampa, FL). Standard curves were generated, correlating pmol of [1-<sup>14</sup>C]-arachidonic acid injected vs. output signal ( $\mu$ V $\cdot$ sec). Extraction efficiencies averaged 75%, estimated by addition of radiolabeled internal standards (8,9-/11,12-EET).

Chemical inhibitors and unlabeled eicosanoids used as reference compounds were from Cayman Chemical Company (Ann Arbor, MI), except for 12-HETrE and 12-oxo-5,8,14-eicosatrienoic acid (12-oxo-ETrE) (from S.G. Jagadeesh and J.R. Falck), *N*-adamantanyl-*N'*-dodecanoic acid urea (from C. Morrisseau and B.D. Hammock), and 1-aminobenzotriazole (Sigma-Aldrich, St. Louis, MO). The [1-<sup>14</sup>C]-EET reference standards were synthesized from [1-<sup>14</sup>C]-arachidonate using 3-chloroperbenzoic acid

JPET #93922

(Sigma-Aldrich, St. Louis, MO), as described (Falck et al., 1990).

Dihydroxyeicosatrienoic acids (DiHETrE) were prepared from EETs as described (Zeldin et al., 1993), by hydrolysis in 50% CH<sub>3</sub>COOH in water for 12-h at 45°C under argon, with constant mixing. Synthesized EETs and DiHETrEs were purified before use by reversed-phase HPLC.

**Liquid chromatography mass spectrometry (LC/MS).** LC/MS analyses were performed using a ThermoElectron LCQ DecaXP (San Jose, CA) ion trap mass spectrometer equipped with an Agilent Technologies (Wilmington, DE) 1100 series binary HPLC pump and thermostated autosampler. Chromatographic separations were done on a 150 x 1.0 mm, 5- $\mu$ m, 300-Å Jupiter C18 column (Phenomenex Inc., Torrance, CA), using a binary acetonitrile/water gradient at flow rate of 75  $\mu$ L/min. Solvent A consisted of acetonitrile/water (5/95; v/v) buffered with 10 mM ammonium acetate at pH 5.5. Solvent B consisted of acetonitrile/water (95/5; v/v) buffered with 10 mM ammonium acetate at pH 5.5. The solvent gradient had an initial isocratic hold for 1 minute at 35% B, followed by a linear gradient program from 35% B to 100% B over 14 minutes, then held at 100% B for 7 minutes. LC/MS experiments were done using negative electrospray ionization (ESI) using the standard DecaXP ESI source; nitrogen was used for both the sheath and auxiliary drying gases. The ESI spray potential was held at 3.5-kV, and the heated capillary ion transfer tube was held at 300°C. An ion source declustering potential of 10-eV was employed to enhance signal intensity. Optimal ESI operating conditions were established using a post-column infusion of arachidonic acid. Full scan spectra were recorded over the mass range m/z 200–400,

JPET #93922

at a scan rate of 1.4 spectra/sec. Product ion spectra were determined in the ion trap over the mass range  $m/z$  75–330 with normalized collision energy of 35%, using data-dependent scanning with a signal intensity threshold of  $5 \times 10^5$  counts. Products were kept at  $-20^\circ\text{C}$  until analysis and then held at  $5^\circ\text{C}$  in the refrigerated autosampler.

Special precautions were taken to prevent isomerization of 12-oxo-ETrE, which was freshly synthesized (by S.G.J. and J.R.F.) the day before analysis and shipped overnight on dry ice to Vanderbilt. Upon arrival, it was immediately diluted in mobile phase and analyzed by LC/MS.

## Results

**Mouse epidermal microsomes generate NADPH-dependent products from arachidonic acid.** Microsomes were prepared from both the epidermis and full-thickness mouse skin; both were active towards [1-<sup>14</sup>C]-arachidonic acid and generated similar product profiles. The majority of [<sup>14</sup>C]-products formed in the absence of NADPH, presumably by epidermal lipoxygenases and cyclooxygenases. However, two products (I and II) formed only in the presence of NADPH, potentially arising from cytochrome P450-dependent catalysis (Fig. 1). Product I had the same retention time as the CYP2B19 product 14,15-EET, resolved by reversed-phase HPLC (Fig. 1A). No products were observed when microsomes were preheated at 65°C for 10-min, indicating the two NADPH-dependent products arise enzymatically (data not shown).

We detected product co-eluting with a single EET regioisomer (14,15-EET), even though epoxygenases including CYP2B19 typically generate two or more EET regioisomers. This could not be explained by epoxide hydrolase-dependent hydrolysis of EET regioisomers to the corresponding vicinal diols. The soluble epoxide hydrolase inhibitor *N*-adamantanyl-*N'*-dodecanoic acid urea (10-100 μM) had no discernable effect on the profile of eicosanoids generated from arachidonate by mouse epidermal microsomes (data not shown). Minor products having similar retention times as authentic DiHETrEs were formed regardless of whether NADPH was added (Fig. 1). There was also no evidence for 5,6-DiHETrE 1,5-lactone, which could be resolved from product I in the reversed-phase HPLC system. We concluded that DiHETrEs were not generated at detectable levels.

JPET #93922

Accumulation of the NADPH-dependent product  $\Gamma$  increased linearly only over 10 min, at protein concentrations up to 1 mg/ml for epidermal microsomes or 4 mg/ml for whole skin microsomes. We reasoned that NADPH-dependents products would be more easily detected if we could eliminate the competition for substrate by epidermal lipoxygenases and cyclooxygenases. However, we were unable to selectively inhibit these NADPH-independent activities towards arachidonate (inhibitor data not shown). At all concentrations tested, the lipoxygenase inhibitors nordihydroguaiaretic acid (2-50  $\mu$ M) and baicalein (0.1-5  $\mu$ M) inhibited at least partially the formation of product  $\Gamma$ . This effect could be nonspecific or it could indicate lipoxygenase activities were involved in product  $\Gamma$  formation. Because the cyclooxygenase inhibitor indomethacin (25-50  $\mu$ M) increased product  $\Gamma$  formation modestly (range: 30%-300%), we routinely preincubated microsomes with 25- $\mu$ M indomethacin, even though this drug had no measurable effect on NADPH-independent product formation. Inexplicably, the partial inhibition of product  $\Gamma$  due to nordihydroguaiaretic acid or baicalein was reversed by preincubating microsomes with both indomethacin and lipoxygenase inhibitor.

To prove whether product  $\Gamma$  was the CYP2B19 product 14,15-EET, a mixture of purified [ $^{14}$ C]-product  $\Gamma$  and [ $^{14}$ C]-14,15-EET was resolved by normal phase HPLC. These entities proved to be chemically distinct (Fig. 2A), a result confirmed by the apparent stability of product  $\Gamma$  in the presence of acetic acid (Fig. 2B). When [1- $^{14}$ C]-14,15-EET was subjected to the same acidic conditions, [1- $^{14}$ C]-14,15-DiHETrE formed (Fig. 2C). Previously we used mass spectrometry to prove that CYP2B19 protein is expressed and that cellular EET accumulates in mouse epidermal keratinocytes (Du et al., 2005). Yet, under the assay conditions epidermal microsomes did not form

JPET #93922

detectable levels of EET. It is not clear whether this was due to low CYP protein levels, instability or deleterious effects of sample preparation on CYP activities, low substrate turnover for epoxygenases relative to lipoxygenases and cyclooxygenases, or substrate depletion due to rapid conversion of arachidonate to NADPH-independent products. If product I was not 14,15-EET, what were the identities of the NADPH-dependent products?

### **Mouse epidermal microsomes generate 12-HETrE from arachidonic acid.**

Spectral data indicated the NADPH-dependent products (I and II) were not conjugated dienes, dienones or trienes since neither had demonstrable absorbance at 237- or 280-nm (Table I). Hydroxyeicosatrienoic acid regioisomers were evaluated since these eicosanoids have similar spectral properties as the epidermal products I and II. Neither of the NADPH-dependent products co-eluted with 15-hydroxy-8,11,13-eicosatrienoic acid (15-HETrE), resolved by reversed-phase HPLC. Product II co-eluted with 12-HETrE (Table 1), an eicosanoid formed from arachidonate by bovine corneal and rat epidermal microsomes (Murphy et al., 1988; Nishimura et al., 1991; Van Wauwe et al., 1991).

To prove whether the intermediates involved in 12-HETrE synthesis were also present in the *in vitro* reactions, we purified products I, II, III and IV (from Fig. 1). Each of these products was mixed individually with a selected reference compound, and the mixtures were resolved on two chromatographic systems. The NADPH-dependent product II was identified as 12-HETrE since it co-eluted with this reference compound on reversed-phase and normal phase HPLC systems (Table 1). Product IV, a major

JPET #93922

NADPH-independent product, was assumed to be HETE because it had an absorbance maximum at 237-nm, indicative of a conjugated diene chromophore. Product IV co-eluted with 12-HETE in both chromatographic systems (Table 1). The minor NADPH-independent product III had an absorbance maximum at 282-nm in our reversed-phase solvent system, indicative of a conjugated dienone chromophore. Product III co-eluted with 12-oxo-ETE in both chromatographic systems (Table 1). Finally, the NADPH-dependent product I, previously shown not to be an epoxy fatty acid, co-eluted with 12-oxo-ETrE in both chromatographic systems (Table 1). We concluded from these chromatographic and spectral data that mouse epidermal microsomes contain competent enzymes that generate all of the intermediates in the 12-HETrE biosynthetic pathway (Fig. 3).

**Mass spectral analyses confirm that mouse epidermal microsomes generate 12-oxo-ETrE and 12-HETrE from arachidonic acid.** We confirmed the structures of the two NADPH-dependent products 12-oxo-ETrE (I) and 12-HETrE (II), using LC/ESI/MS (Fig. 4). The LC elution time and ESI tandem mass spectrum of product II were identical to those obtained for authentic 12-HETrE (Fig. 4A-D). In addition to the carboxylate anion  $[M-H]^-$  at  $m/z$  321 and its dehydration product  $[M-H-H_2O]^-$  at  $m/z$  303, the two abundant ions  $m/z$  181 and 209 are indicative of hydroxyl position in 12-HETrE/product II. The inset indicates the cleavage and ion structure for these two ions (Fig. 4D). Likewise, Fig. 4E-H shows identical LC elution times and ESI tandem mass spectra for product I and authentic 12-oxo-ETrE. Ions at  $m/z$  319, 301, and 275 represent the carboxylate anions  $[M-H]^-$ ,  $[M-H-H_2O]^-$ , and  $[M-H-CO_2]^-$ ,

JPET #93922

respectively. Structures for ions  $m/z$  163 and 153 are shown in the inset; ion  $m/z$  163 may result from internal cleavages as indicated (Fig. 4H).

As a positive control, we also analyzed product *IV*, identified as 12-HETE (Table 1). The LC elution time and ESI tandem mass spectrum of product *IV* were identical to those for authentic 12-HETE (data not shown). We did not subject product *III*/12-oxo-ETE to LC/MS due to the small mass of this intermediate that accumulates in the reaction mixture. These LC/MS data and the chromatographic and spectral properties of the epidermal [ $^{14}\text{C}$ ]-products as shown in Table 1 are in agreement and confirm the proposed structural identities of products *I*, *II*, *III*, and *IV*. These are: 12-oxo-ETrE, 12-HETrE, 12-oxo-ETE, and 12-HETE, respectively.

**Evidence that lipoxygenases in mouse epidermal microsomes, rather than cytochromes P450, have major roles in 12-HETrE biosynthesis.** To investigate precursor-product relationships, we measured the accumulation of epidermal [ $^{14}\text{C}$ ]-products *I*, *II*, *III*, and *IV* over time, in the presence of NADPH (Fig. 5). 12-Hydroxyeicosatetraenoic acid (*IV*) was by far the most abundant product. The mass of 12-HETE increased continuously for 40 min, indicating 12-HETE is the major end product of this reaction (Fig. 5A). The second most abundant product measured was 12-hydroperoxy eicosatetraenoic acid (12-HpETE), the immediate product of 12-lipoxygenase. However, the mass of 12-HpETE decreased after 10-min, to very low levels. The mass of 12-HETrE (*II*) increased continuously over 40 min, indicating 12-HETrE is also an end product (Fig. 5A and expanded scale in Fig. 5B). The initial increase in 12-oxo-ETE (*III*) and 12-oxo-ETrE (*I*) accumulation slowed markedly or

JPET #93922

began to decrease after 10 min, resembling the pattern observed for 12-HpETE, consistent with their roles as metabolic intermediates.

Two end products formed from arachidonate--12-HETE and lesser amounts of 12-HETrE (Fig. 5). To ascertain whether CYP proteins were involved in their synthesis, we used 1-aminobenzotriazole, a mechanism-based inhibitor of cytochrome P450 having low isoform selectivity. Pretreatment of mouse epidermal microsomes with 100-1000  $\mu$ M of 1-aminobenzotriazole did not selectively block NADPH-dependent product formation (data not shown), nor could we detect a measurably decrease in 12-HETE accumulation. We conclude that epidermal lipoxygenases, rather than CYP proteins, likely have prominent roles in 12-HETrE synthesis, along with other unidentified enzymes responsible for the NADPH-dependent conversion of 12-oxo-ETE to 12-oxo-ETrE and 12-HETrE.

## Discussion

Regioisomeric EETs generated from endogenous arachidonic acid are present in mouse epidermal tissue and differentiating epidermal cell cultures, indicating the presence of catalytically active epoxygenases (Keeney et al., 1998; Du et al., 2005). As existing evidence suggests mouse CYP2B19 is mainly responsible for cellular EET formation in mouse skin (Du et al., 2005), we set out to demonstrate that this keratinocyte-specific epoxygenase in epidermal microsomes is responsible for generating EETs from [1-<sup>14</sup>C]-arachidonate *in vitro*. Instead of EET formation, we identified a NADPH-dependent pathway leading to biosynthesis of 12-HETrE. This is the first report showing this pathway is active in mouse skin.

A novel feature of mouse epidermal microsomes is that we were able to identify and characterize all four intermediates in synthesis of 12-HETrE from arachidonate: 12-HETE/12-HpETE, 12-oxo-ETE, and 12-oxo-ETrE. Second, we found no evidence for formation of 15-hydroxyeicosatrienoic acid isomers, unlike rat epidermal microsomes, which generate 15-hydroxy-5,8,11-eicosatrienoic acid from arachidonate (Van Wauwe et al., 1991, 1992). This might represent a species difference or the levels of this regioisomer were just too low to be detected in our assay system. In human skin, HETrE formation has been reported from dietary polyunsaturated fatty acid, but not from arachidonic acid. For example, human epidermal cells can generate 15-hydroxy-8,11,13-eicosatrienoic acid from  $\gamma$ -linolenic acid (Ziboh et al., 2000).

Even though EET biosynthesis was not detected *in vitro*, CYP2B19 is expressed in mouse epidermal keratinocytes; CYP2B19-derived peptides were identified

JPET #93922

unequivocally by mass spectrometry, following immunoaffinity chromatography (Du et al., 2005). In addition to explanations already discussed why EET biosynthesis was not detected, we question whether epidermal epoxygenases utilize exogenous arachidonic acid efficiently in the microsomal environment. Cyclooxygenase (*PTGS1* and *PTGS2*) activity levels differed depending on whether substrate was exogenous or endogenous arachidonic acid (Chulada et al., 1996). In our system, exogenous arachidonate was utilized much more efficiently by epidermal lipoxygenases and cyclooxygenases, than epoxygenases. Even though soluble and microsomal epoxide hydrolases are expressed in the epidermis (Winder et al., 1993), we found little evidence for hydrolysis of EETs to vicinal diols using an inhibitor of soluble epoxide hydrolase--the form mainly responsible for hydrolysis of epoxy fatty acids (Newman et al., 2005).

The NADPH-dependent products I and II (12-oxo-ETrE and 12-HETrE, respectively) appeared to form at the expense of product III (12-oxo-ETE). This was the first evidence for a precursor-product relationship. The time dependent accumulation and disappearance of epidermal [<sup>14</sup>C]-products (I-IV) lend credibility to the idea that HETrE biosynthesis in mouse epidermal microsomes shares some of the same intermediates as reported for bovine corneal and rat epidermal microsomes (Van Wauwe et al., 1992; Yamamoto et al., 1994). In the mouse epidermal microsome system, we identified 12-HETE and 12-HETrE as end products, and 12-oxo-ETE and 12-oxo-ETrE as intermediates in the formation of 12-HETrE.

Mechanistically, 12-HETrE synthesis could involve lipoxygenases and/or cytochromes P450 (Nishimura et al., 1991; Van Wauwe, 1991, 1992; Yamamoto et al., 1994). CYP4B1 has been implicated in 12-HETrE formation in the cornea (Mastyugin et

JPET #93922

al., 1999). We were unable to establish specific evidence implicating a CYP protein in 12-HETrE formation, but neither could we specifically rule out this possibility.

Epidermal 12-lipoxygenase activities were likely involved in 12-oxo-ETE biosynthesis since highest levels of this intermediate were observed in the absence of NADPH. Of six functional lipoxygenase genes in humans and seven in mice, several including platelet-type and epidermis-type 12*S*-lipoxygenase and 12*R*-lipoxygenase are expressed in skin, potentially contributing to 12-oxo-ETE formation (de Laclos et al., 1987; Yoshimoto and Takahashi, 2002; Antón and Vila, 2000; Funk et al., 2002). That 12-HETE was the most abundant end product is consistent with previous studies establishing 12-lipoxygenase as the major lipoxygenase activity in mouse skin microsomes (Nakadate et al., 1986).

Enzymes responsible for the NADPH-dependent conversion of 12-oxo-ETE to 12-oxo-ETrE and 12-HETrE have not been studied in the epidermis. However, in porcine leukocytes a microsomal NAD<sup>+</sup>-dependent dehydrogenase activity was characterized that generates 12-oxo-ETE from 12-HETE. This oxidation step was prerequisite for maximal activity of a cytosolic NADH-dependent 10,11-reductase (Wainwright et al., 1990; Wainwright and Powell, 1991). Involvement of a cytosolic reductase in mouse epidermis is contradicted by the observation that microsomes prepared from epidermis and full-thickness skin (epidermis and dermis) were competent to generate 12-HETrE; however, we cannot rule out minor cytosolic contamination. The 12-/15-oxo-ETE, and 12-/15-oxo-ETrE intermediates are common to diverse cell systems, suggesting that pathways for HETrE are conserved in mammalian skin, cornea, leukocytes, and quite possibly many other tissues. Important differences might

JPET #93922

be found in the mechanisms regulating production of regioisomeric HETrEs or biologically active intermediates.

In differentiating keratinocytes, CYP-derived EETs are implicated in mechanisms regulating transglutaminase enzyme activities, which are critical for normal epidermal cornification (Ladd et al., 2003). Is epidermal HETrE biosynthesis physiological relevant? In the cornea, 12*R*-HETrE formation is enhanced by injury and hypoxia, and its proinflammatory properties include vasodilation of blood vessels, neutrophil chemoattraction, endothelial cell proliferation and neovascularization (Murphy et al., 1988; Stoltz and Schwartzman, 1997). Both 12-HETE enantiomers are substrate for 12-HETrE biosynthesis, but only 12*R*-HETrE has significant proinflammatory properties (Yamamoto et al., 1994; Stoltz and Schwartzman, 1997). In guinea pig skin, 12*R*-HETrE is also proinflammatory, enhancing delayed-type hypersensitivity inflammatory reactions at dosages as low as 1 fmol (Connors et al., 1995). Neither of the 12-HETE enantiomers or 12*S*-HETrE had this activity.

The extent that epidermally-derived 12-HETE serves as precursor for 12-HETrE biosynthesis in human skin is unknown since this pathway has not been studied in human epidermal cells, nor have cellular 12-HETrE levels been reported for normal or diseased skin. In hyperproliferative dermatoses (e.g., psoriatic), 12-HETE accumulates to greater levels in lesional (vs. normal) skin (Hammarström et al., 1979). The 12*R*-HETE enantiomer predominates and is more chemotactic (Woollard, 1986; reviewed by: Ikai, 1999; Fogh and Kragballe, 2000).

Results of recent studies suggest the proinflammatory activities of 12-HETrE are counterbalanced by the anti-inflammatory and anti-proliferative activities of 15-HETrE

JPET #93922

(Ziboh et al., 2000) and that these lipid mediators may utilize different signaling mechanisms. High affinity binding sites characterized in microvessel endothelial cells potentially mediate the proinflammatory actions of 12*R*-HETrE (Stoltz and Schwartzman, 1997). The 15-HETrE regioisomer was found incorporated into phospholipids, and when released by phospholipase C as 15-HETrE-diacylglycerol, this lipid moiety modulated protein kinase C activities (reviewed by Ziboh et al., 2000).

Important future studies are to establish whether 12-/15-HETrE biosynthetic pathways are operative in human epidermal cells, to characterize the regio- and stereochemistry of the eicosanoids formed and their biological activities in human skin. Opposing pro- and anti-inflammatory activities for 12- and 15-HETrE make sense biologically, to regulate cutaneous inflammatory and immune responses. In this regard, it was proposed that 15-HETE might influence the development of psoriatic lesions by its ability to inhibit synthesis of the proinflammatory lipids 5- and 12-HETE (reviewed by Ikai, 1999). Again, it is unclear to what extent lipoxygenase-derived products are utilized as precursor for hydroxyeicosatrienoic acid biosynthesis or to what extent this secondary metabolism contributes to observed biological effects. In addition to modulating cutaneous inflammatory responses, it seems likely that regioisomeric HETrEs and biosynthetic intermediates have additional activities that remain to be discovered.

JPET #93922

## Acknowledgments

The authors thank Patricia Ladd for assistance with mouse epidermal preparations; Drs. Bruce Hammock and Christophe Morrisseau for epoxide hydrolase inhibitor; Shouzou Wei and Drs. Alan Brash, Jorge Capdevila, John Newman, and Claus Schneider for advice and expertise in eicosanoid analyses and critical discussions of the data.

## References

- Antón R and Vila L (2000) Stereoselective biosynthesis of hepoxilin B3 in human epidermis. *J Invest Dermatol* **114**:554-559.
- Bedford, CJ, Young JM, Wagner, BM (1983) Anthralin inhibition of mouse epidermal arachidonic acid lipoxygenase in vitro. *J Invest Dermatol* **81**:566-571.
- Cameron GS, Baldwin, JK, Jasheway DW, Patrick KE, and Fischer SM (1990) Arachidonic acid metabolism varies with the state of differentiation in density gradient-separated mouse epidermal cells. *J Invest Dermatol* **94**:292-296.
- Capdevila JH, Falck JR, Dishman E, and Karara A (1990) Cytochrome P-450 arachidonate oxygenase. *Methods Enzymol* **187**:385-94.
- Capdevila JH, and Falck JR (2002) Cytochrome P450 and arachidonic acid bioactivation: molecular and functional properties of the arachidonate monooxygenases. *Prostaglandins Other Lipid Mediators* **68-69**:325-344.
- Chulada PC, Loftin CD, Winn WD, Young DA, Tiano HF, Eling TE, and Langenbach R (1996) Relative activities of retrovirally expressed murine prostaglandin synthase-1 and -2 depend on source of arachidonic acid. *Archiv Biochem Biophys* **330**:301-313.
- Connors MS, Schwartzman ML, Quan X, Heilman E, Chauhan K, Falck JR, and Godfrey HP (1995) Enhancement of delayed hypersensitivity inflammatory reactions in guinea pig skin by 12(*R*)-hydroxy-5,8,14-eicosatrienoic acid. *J Invest Dermatol* **104**:47-51.
- De Lacos BF, Maclouf J, Poubelle, P, and Borgeat P (1987) Conversion of arachidonic

JPET #93922

acid into 12-oxo derivatives in human platelets. A pathway possibly involving the heme-catalyzed transformation of 12-hydroperoxyeicosatetraenoic acid.

*Prostaglandins* **33**:315-337.

Du L, Yermalitsky V, Ladd PA, Capdevila JH, Mernaugh R, and Keeney DS (2005)

Evidence that cytochrome P450 CYP2B19 is the major source of

epoxyeicosatrienoic acids in mouse skin. *Arch Biochem Biophys* **435**:125-133.

Falck JR, Yadagiri P, and Capdevila J (1990) Synthesis of epoxyeicosatrienoic acids

and heteroatom analogs. *Methods Enzymol* **187**:385-394.

Fogh K, and Kragballe K (2000) Eicosanoids in inflammatory skin diseases.

*Prostaglandins Other Lipid Mediators* **63**:43-54.

Funk CD, Chen X-S, Johnson EN, and Zhao L (2002) Lipoxygenase genes and their

targeted disruption. *Prostaglandins Other Lipid Mediators* **68-69**:303-312.

Hammarström S, Lindgren JA, Marcelo CL, Duell EA, Anderson TF, Voorhees JJ (1979)

Arachidonic acid transformations in normal and psoriatic skin. *J Invest Dermatol*

**73**:180-183.

Henke D, Danilowicz R, and Eling T (1986) Arachidonic acid metabolism by isolated

epidermal basal and differentiated keratinocytes from the hairless mouse. *Biochim*

*Biophys Acta* **876**:271-279.

Holtzman MJ, Turk J, and Pentland A (1989) A regiospecific monooxygenase with novel

stereopreference is the major pathway for arachidonic acid oxygenation in isolated

epidermal cells. *J Clin Invest.* **84**:1446-1453.

Ikai K (1999) Psoriasis and the arachidonic acid cascade. *J Dermatol Sci* **21**:35-146.

Iversen L and Kragballe K (2000) Arachidonic acid metabolism in skin health and

JPET #93922

disease. *Prostaglandins Other Lipid Mediators* **63**:25-42.

Kabashima K, and Miyachi Y (2004) Prostanoids in the cutaneous immune response. *J Dermatol Sci* **34**:177-184.

Keeney DS, Skinner C, Travers JB, Capdevila JH, Nanney LB, King LE Jr, and Waterman, MR (1998) Differentiating keratinocytes express a novel cytochrome P450 enzyme, CYP2B19, having arachidonate monooxygenase activity. *J Biol Chem* **273**:32071-32079.

Ladd PA, Du L, Capdevila JH, Mernaugh R, and Keeney DS (2003) Epoxyeicosatrienoic acids activate transglutaminases *in situ* and induce cornification of epidermal keratinocytes. *J Biol Chem* **278**:35184-35192.

Marks F, Müller-Decker K, and Fürstenberger G (2000) A causal relationship between unscheduled eicosanoid signaling and tumor development: cancer chemoprevention by inhibitors of arachidonic acid metabolism. *Toxicol Letters* **153**:11-26.

Mastyugin V, Aversa E, Bonazzi A, Vafaes C, Mieyal P, and Schwartzman ML (1999) Hypoxia-induced production of 12-hydroxyeicosanoids in the corneal epithelium: involvement of a cytochrome P-450B1 isoform. *J Pharmacol Exp Ther* **289**:1611-1619.

Murphy RC, Falck JR, Lumin S, Yadagiri P, Zirrolli JA, Balazy M, Masferrer JL, Abraham NG, and Schwartzman ML (1988) 12(*R*)-hydroxyeicosatrienoic acid: a vasodilator cytochrome P-450-dependent arachidonate metabolite from the bovine corneal epithelium. *J Biol Chem* **263**:17197-17202.

Nakadate T, Aizu E, Yamamoto S, and Kato R (1986) Some properties of lipoxygenase activities in cytosol and microsomal fractions of mouse epidermal homogenate.

JPET #93922

*Prostaglandins Leukotrienes Med* **21**:305-319.

Nebert DW, and Russell DW (2002) Clinical importance of the cytochromes P450.

*Lancet* **360**:1155-1162.

Nelson DR, Zeldin DC, Hoffman SMG, Maltais LJ, Wain HM, and Nebert DW (2004)

Comparison of cytochrome P450 (*CYP*) genes from the mouse and human genomes, including nomenclature recommendations for genes, pseudogenes, and alternative-splice variants. *Pharmacogenetics* **14**:1-18.

Newman JW, Morisseau C, and Hammock BD (2005) Epoxide hydrolases: their roles and interactions with lipid metabolism. *Prog Lipid Res* **44**:1-51.

Nishimura M, Schwartzman ML, Falck JR, Lumin S, Zirrolli JA, and Murphy RC (1991)

Metabolism of 12(*R*)-hydroxy-5,8,10,14-eicosatetraenoic acid (12(*R*)-HETE) in corneal tissues: formation of novel metabolites. *Arch Biochem Biophys* **290**:326-335.

Ruzicka T, Walter JF, and Printz MP (1983) Changes in arachidonic acid metabolism in UV-irradiated hairless mouse skin. *J Invest Dermatol* **81**:300-303.

Stoltz RA, and Schwartzman ML (1997) High affinity binding sites for 12(*R*)-

hydroxyeicosatrienoic acid [12(*R*)-HETrE] in microvessel endothelial cells. *J Ocular Pharmacol* **13**:191-199.

Van Wauwe J, Coene M-C, Van Nyen G, Cools W, Goossens J, Le Jeune L, Lauwers W, and Janssen PAJ (1991) NADPH-dependent formation of 15- and 12-

hydroxyeicosatrienoic acid from arachidonic acid by rat epidermal microsomes. *Eicosanoids* **4**:155-163.

Van Wauwe J, Coene M-C, Van Nyen G, Cools W, Le Jeune L, and Lauwers W (1992)

Suggested mechanism for the formation of 15-hydroxyeicosatrienoic acid by rat

JPET #93922

epidermal microsomes. *Eicosanoids* **5**:141-146.

Wainwright S, Falck JR, Yadagiri P, and Powell WS (1990) Metabolism of 12(S)-hydroxy-5,8,10,14-eicosatetraenoic acid and other hydroxylated fatty acids by the reductase pathway in porcine polymorphonuclear leukocytes. *Biochemistry* **29**:10126-10135.

Wainwright SL, and Powell WS (1991) Mechanism for the formation of dihydro metabolites of 12-hydroxyeicosanoids. *J Biol Chem* **266**:20899-20906.

Winder BS, Nourooz-Zadeh J, Isseroff RR, Moghaddam MF, and Hammock BD (1993) Properties of enzymes hydrating epoxides in human epidermis and liver. *Int J Biochem* **25**:1291-1301.

Woollard PM (1986) Stereochemical difference between 12-hydroxy-5,8,10,14-eicosatetraenoic acid in platelets and psoriatic lesions. *Biochem Biophys Res Comm* **136**:169-176.

Yamamoto S, Nishimura M, Connors MS, Stoltz RA, Falck JR, Chauhan K, and Schwartzman ML (1994) Oxidation and keto reduction of 12-hydroxy-5,8,10,14-eicosatetraenoic acid in bovine corneal epithelial microsomes. *Biochem Biophys Acta* **1210**:217-225.

Yoshimoto T, and Takahashi Y (2002) Arachidonate 12-lipoxygenases. *Prostaglandins Other Lipid Mediators* **68-69**:245-262.

Zeldin DC, Kobayashi J, Falck JR, Winder BS, Hammock BD, Snapper JR, and Capdevila JR (1993) Regio- and enantiofacial selectivity of epoxyeicosatrienoic acid hydration by cytosolic epoxide hydrolase. *J Biol Chem* **268**:6402-6407.

JPET #93922

Ziboh VA, Miller CC, and Cho Y (2000) Significance of lipoxygenase-derived monohydroxy fatty acids in cutaneous biology. *Prostaglandins Other Lipid Mediators* **63**:3-13.

JPET #93922

## Footnotes

\*This work was supported in part by resources and funding from the Department of Veterans Affairs and PHS grants NIAMS AR45603 and AR47357 (to D.S.K.); NIGMS GM31278 and the Robert A. Welch Foundation (to J.R.F.); and the Center in Molecular Toxicology at Vanderbilt (NIEHS P30 ES00267).

## Legends for Figures

**Figure 1.** Reversed-phase HPLC chromatograms showing NADPH-dependent formation of two eicosanoids by mouse epidermal microsomes. Reactions were initiated by adding NADPH (**A.**) or vehicle (**B.**) to microsomes reconstituted at 2.0 mg/ml in the presence of 100- $\mu$ M [1- $^{14}$ C]-arachidonate. The NADPH-dependent products I and II and the NADPH-independent products III and IV were selected for further study. Product I (22.9 min) was clearly resolved and eluted with authentic 14,15-EET. The lag time between UV and radioactivity detectors was  $0.5 \pm 0.1$  min, and elution times for relevant unlabeled reference compounds were ( $\pm 0.2$  min): prostaglandin E<sub>2</sub>, 4.5 min; 14,15-, 11,12-, 8,9-, and 5,6-DiHETrE, 10-13 min; 20-HETE, 14.3 min; 15-HETE, 17.1 min; 8-/12-HETE, 18.5 min; 5-HETE, 19.5 min; 5,6-DiHETrE 1,5-lactone, 21.3; 14,15-EET, 22.0 min; 11,12-/8,9-EET, 23.0-23.5; 5-hydroxy-6,8,11,14-eicosatetraenoic acid 1,5-lactone, 30.4 min; arachidonate, 31.8 min.

**Figure 2.** Evidence that the NADPH-dependent epidermal product I is distinct from 14,15-EET. **A.**, a mixture containing purified [ $^{14}$ C]-product I and authentic [ $^{14}$ C]-14,15-EET and [ $^{14}$ C]-arachidonic acid was subjected to normal phase HPLC (NP-HPLC). The three compounds eluted at 25.6, 22.7, and 8.4, min, respectively, indicative of three distinct chemical entities. **B.-C.**, purified [ $^{14}$ C]-product I was subjected to reversed-phase HPLC (RP-HPLC) after overnight incubation in 50% acetic acid. Its elution time was unchanged by this treatment (22.9 min), evidence that product I is not an epoxy fatty acid. Under the same conditions, the elution time for authentic [ $^{14}$ C]-14,15-EET

JPET #93922

shifted to 12.2 min, indicating hydrolysis to [ $^{14}\text{C}$ ]-14,15-DiHETrE. The closed and open arrows indicate elution times for the reference compounds [ $^{12}\text{C}$ ]-14,15-DiHETrE (11.7 min) and [ $^{14}\text{C}$ ]-14,15-EET (22.9 min), respectively.

**Figure 3.** Schematic showing intermediates generated by mouse epidermal microsomes leading to 12-HETrE formation from arachidonic acid (AA). The epidermal products I, II, III and IV are ordered to depict a proposed metabolic pathway, based on results described previously for rat epidermal and bovine corneal microsomes (Van Wauwe, 1992; Yamamoto et al., 1994). Arrows with broken lines represent a minor role for CYP proteins in 12-HETE synthesis since the majority of 12-HETE/12-HpETE (product IV) is formed in the absence of NADPH. “+NADPH” denotes that the next product in the pathway does not form if NADPH is absent.

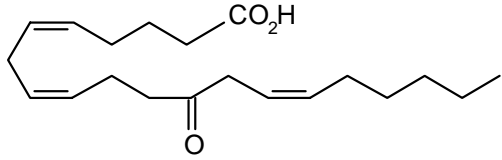
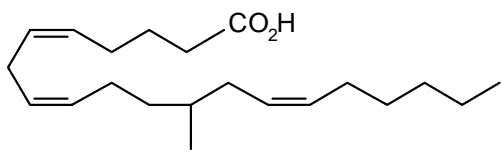
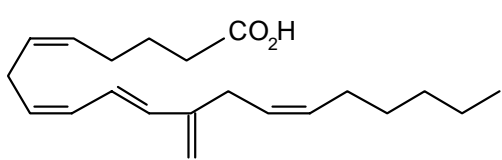
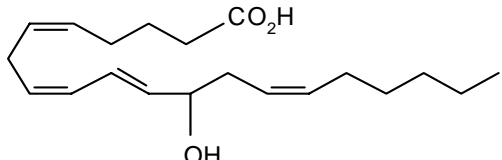
**Figure 4.** LC/MS analyses confirm that the structure of the NADPH-dependent product II is 12-HETrE and product I is 12-oxo-ETrE. **A., C., E., and G.,** total ion chromatograms. **B., D., F., and H.,** tandem ESI mass spectra. Retention times for carboxylate anions  $[\text{M-H}]^-$  derived from purified product II (**A.**) and 12-HETrE (**C.**) are shown in the total ion chromatograms, for the tandem MS product ions of  $m/z$  321; those for purified product I (**E.**) and 12-oxo-ETrE (**G.**) are shown for the tandem MS product ions of  $m/z$  319. Tandem ESI mass spectra show  $[\text{M-H}]^-$  ions derived from product II (**B.**), 12-HETrE (**D.**), product I (**E.**), and 12-oxo-ETrE (**H.**). Insets show the structural formula and deduced fragmentations in the ion trap for 12-HETrE (**D.**) and 12-oxo-ETrE (**H.**).

JPET #93922

**Figure 5.** Rate of product formation by mouse epidermal microsomes reconstituted in the presence of [1-<sup>14</sup>C]-arachidonate. Aliquots of the reaction mixtures were extracted, and the eicosanoids were resolved by reversed-phase HPLC. **A.**, pmol of product was measured at 10, 20, and 40 min after initiating reactions with NADPH. In this experiment only, the proportion of 12-HpETE and 12-HETE in the [<sup>14</sup>C]-product IV fraction was estimated and plotted separately. **B.**, a subset of the data in **A.** is shown using an expanded Y-axis. The symbols are the same as in **A.** **C.**, 12-HpETE and 12-HETE were not resolved in the radiochromatograms (left trace). However, these eicosanoids were resolved spectrally using a diode array detector (right trace), which plotted each compound at the respective  $\lambda_{\text{max}}$  (236.8-nm for 12-HETE; 238.0-nm for 12-HpETE). The contribution of [<sup>14</sup>C]-12-HpETE and [<sup>14</sup>C]-12-HETE in the product IV fraction was estimated by multiplying pmol of [<sup>14</sup>C]-product IV by the proportion of the total area (from UV spectrum) represented by 12-HETE (black arrow) and 12-HpETE (gray arrow).

JPET #93922

**Table 1.** Identity of products generated from [1-<sup>14</sup>C]-arachidonate by mouse epidermal microsomes.

<sup>a</sup> Sample Mixture	Retention Time (min)		$\lambda_{\text{max}}$ (nm)	Structure of Reference Compound
	RP-HPLC	NP-HPLC		
[ <sup>14</sup> C]-Product I + [ <sup>12</sup> C]-12-oxo-ETrE	22.9 22.6	20.5 20.0	<200 <200	
[ <sup>14</sup> C]-Product II + [ <sup>12</sup> C]-12-HETrE	20.5 20.0	20.4 19.9	<200 <200	
[ <sup>14</sup> C]-Product III + [ <sup>12</sup> C]-12-oxo-ETE	20.0 19.5	24.7 24.3	<sup>b</sup> 281.6 <sup>b</sup> 281.6	
[ <sup>14</sup> C]-Product IV + [ <sup>12</sup> C]-12-HETE	18.6 18.1	21.3 20.8	236.8 236.8	

Downloaded from jpet.aspetjournals.org at ASPET Journals on April 19, 2024

JPET #93922

<sup>a</sup>Purified radiolabeled products (I, II, III, IV) were mixed with unlabeled authentic standards, and the mixtures were resolved by reversed-phase (RP) and normal phase (NP) HPLC. The lag time between UV and radioactivity detectors is  $0.5 \pm 0.1$  min.

<sup>b</sup>The composition of the reversed-phase gradient system was water/acetonitrile/acetic acid (24.95/74.95/0.1; v/v/v).

# Figure 1

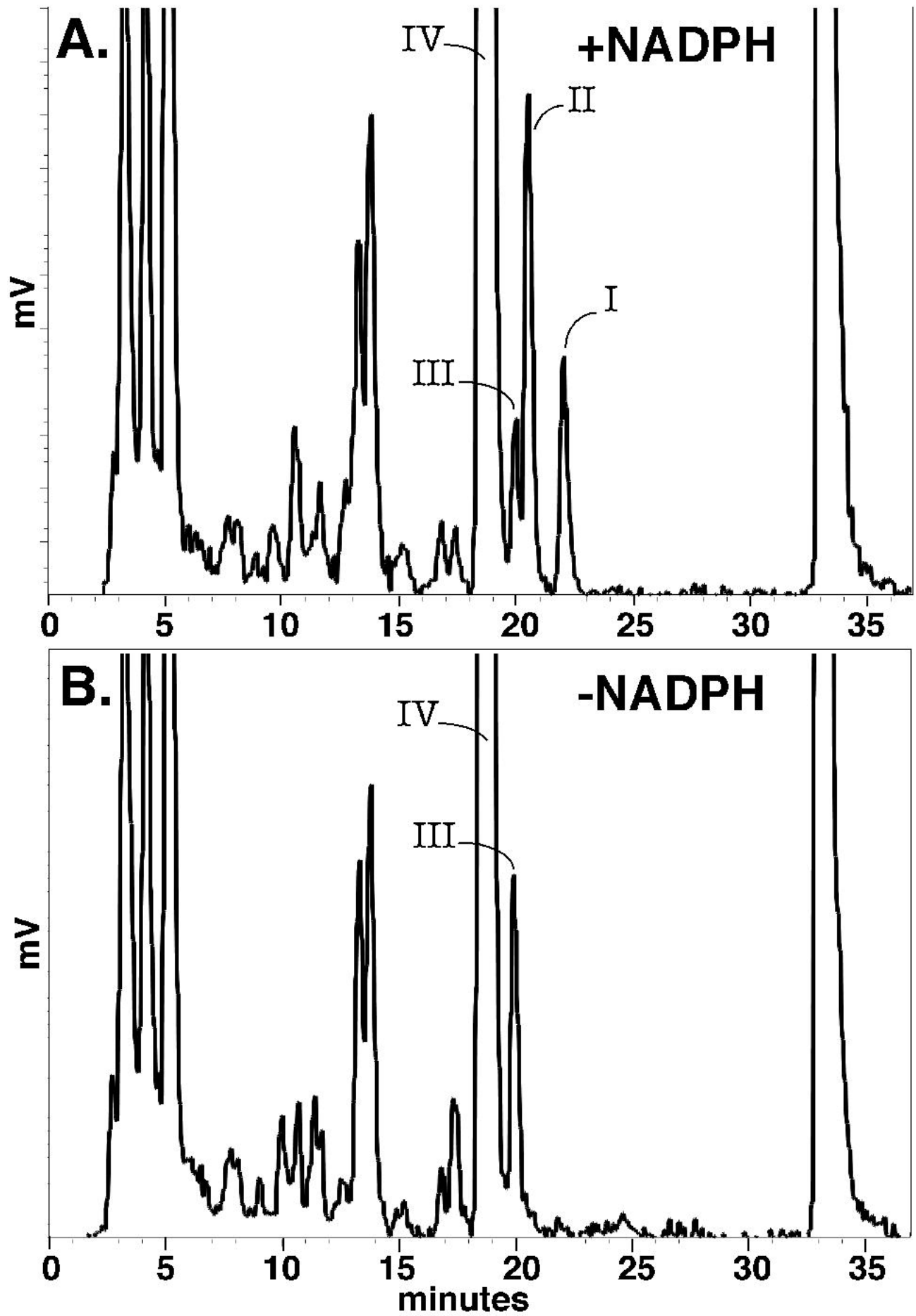


Figure 2

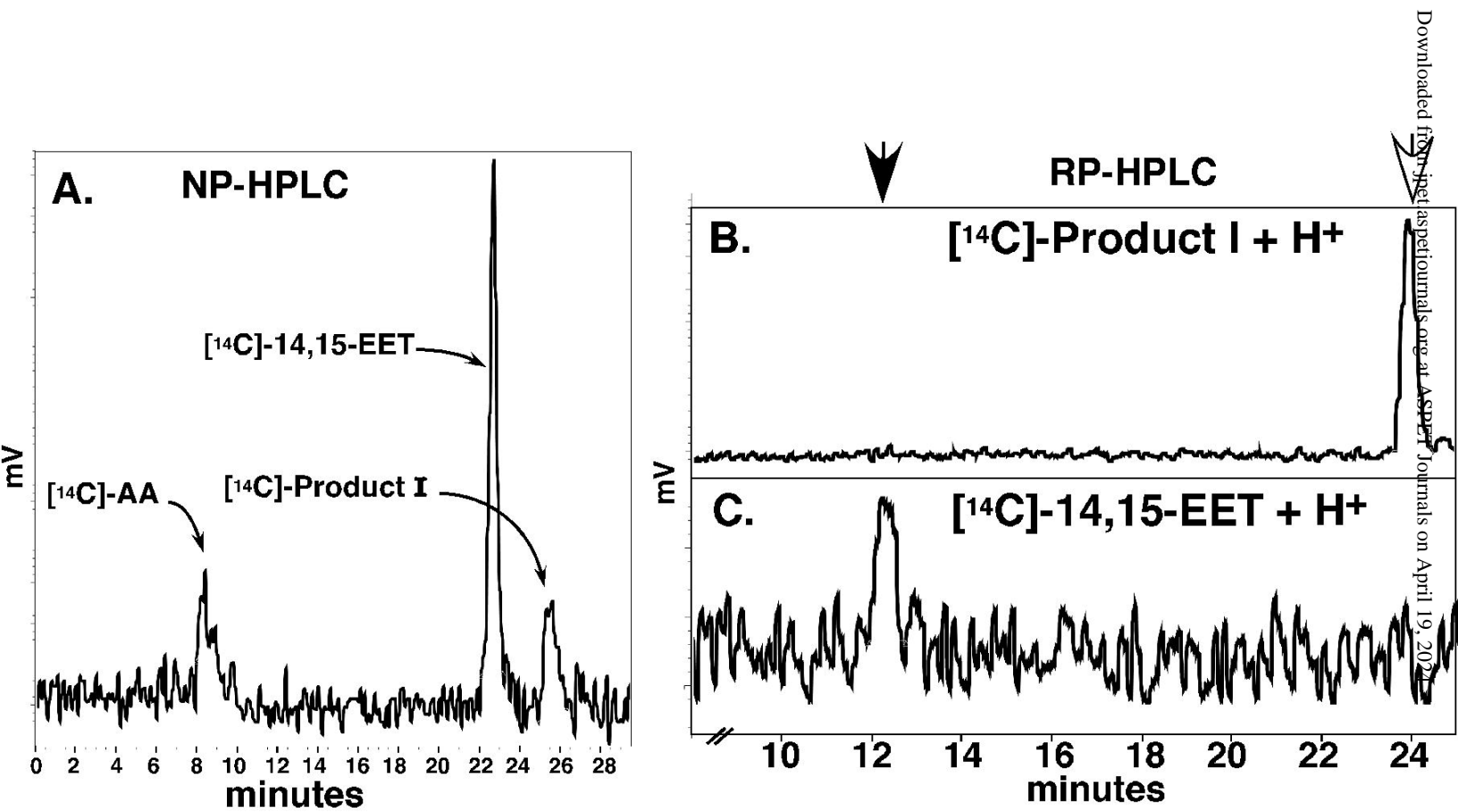


Figure 3

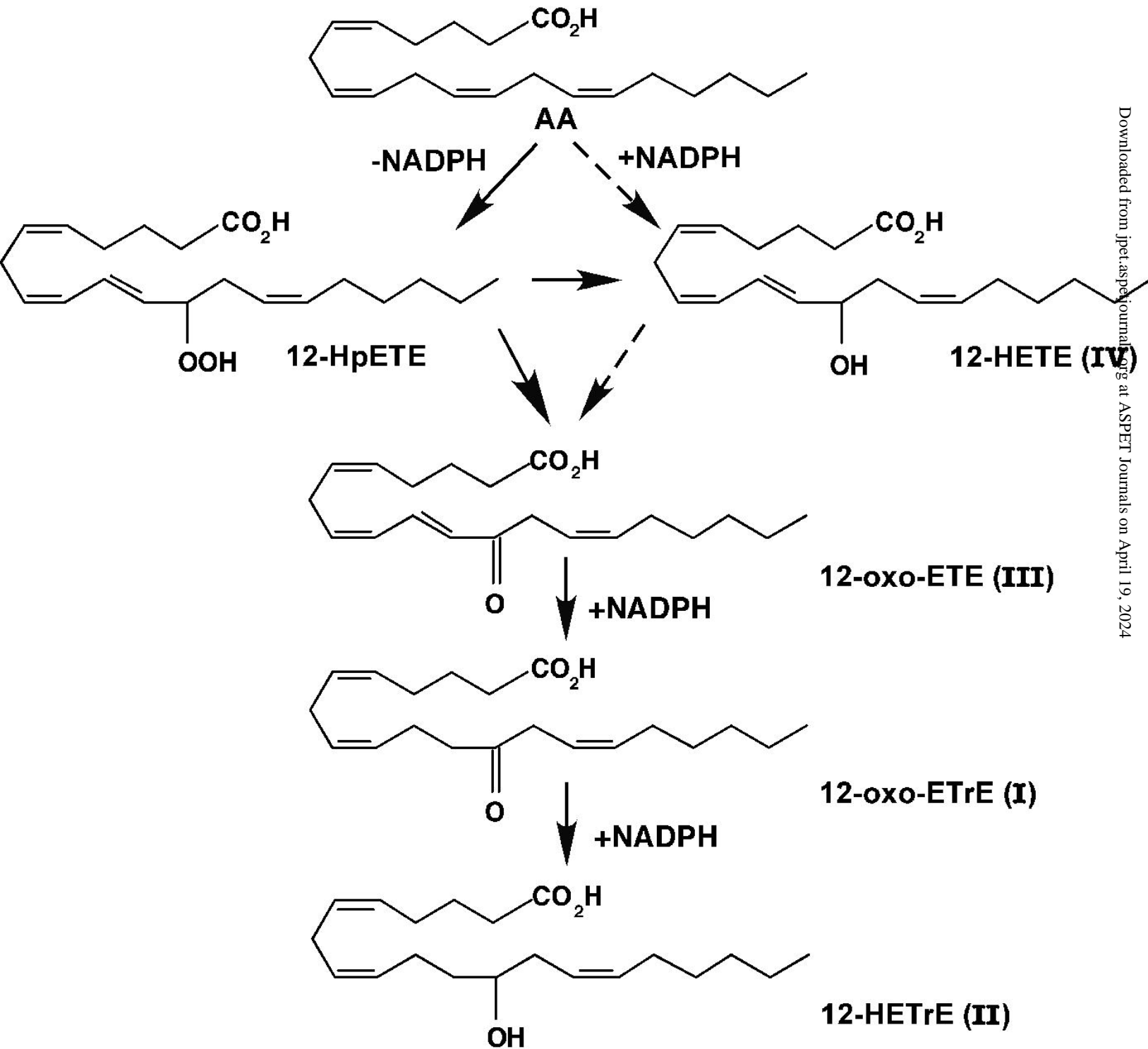


Figure 4

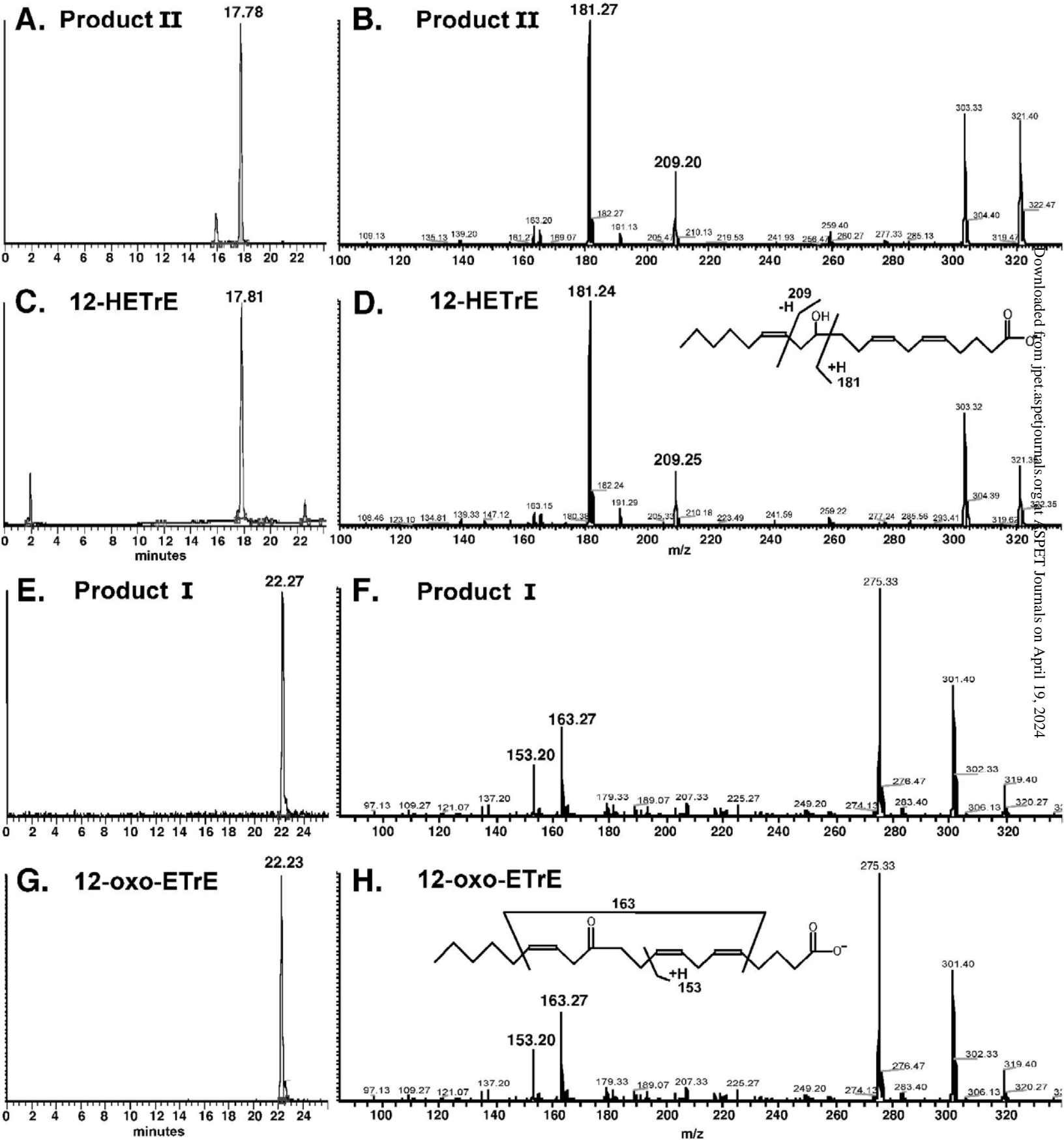


Figure 5

